

CONF-851217--15

By acceptance of this article, the publisher or recipient acknowledges the U.S. Government's right to retain a nonexclusive, royalty-free license in and to any copyright covering the article.

AMORPHIZATION AND RECRYSTALLIZATION PROCESSES IN
MONOCRYSTALLINE BETA SILICON CARBIDE THIN FILMS

- J.A. EDMOND, S.P. WITHROW*, H.S. KONG, AND R.F. DAVIS
• Department of Materials Engineering, North Carolina State University,
Raleigh, NC 27695-7907
*Solid State Division, Oak Ridge National Laboratory, Oak Ridge, TN 37831

CONF-851217--15

ABSTRACT

DE86 004797

Individual, as well as multiple doses of $^{27}\text{Al}^+$, $^{31}\text{P}^+$, $^{28}\text{Si}^+$, and $^{28}\text{Si}^+$ and $^{12}\text{C}^+$ were implanted into (100) oriented monocrystalline β -SiC films. The critical energy of ≈ 16 eV/atom required for the amorphization of β -SiC via implantation of $^{27}\text{Al}^+$ and $^{31}\text{P}^+$ was determined using the TRIM84 computer program for calculation of the damage-energy profiles coupled with the results of RBS/ion channeling analyses. In order to recrystallize amorphized layers created by the individual implantation of all four ion species, thermal annealing at 1600, 1700, or 1800°C was employed. Characterization of the recrystallized layers was performed using XTEM. Examples of SPE regrown layers containing; 1) precipitates and dislocation loops, 2) highly faulted-microtwinned regions, and 3) random crystallites were observed.

INTRODUCTION

The processing steps leading to the development of selected electronic devices in cubic (beta) Silicon Carbide (β -SiC) thin films involve ion implantation to introduce electrically active dopants. As the dose of the implanted specie is increased, the near surface region of this compound semiconductor becomes progressively damaged; atomic disorder and eventual amorphization of the structure occurs. Early work by Hart et al. [1] utilized Rutherford Backscattering (RBS)/channeling techniques in order to study both disorder production in monocrystalline α -SiC by ion implantation and the subsequent thermal annealing of that damage. Williams et al. [2] have previously considered structural alteration in monocrystalline (0001) α -SiC as a result of Cr^+ and N^+ implantation. These authors have made direct comparisons of the theoretical damage profiles calculated using the computer codes E-DEP-1 [3] and TRIM [4] with those determined by RBS/channeling on experimentally implanted SiC samples. From the N^+ implant results, it was determined that the critical-energy-density (CED) for randomization in their material was ≈ 13 eV/atom (randomized regions refer to areas in the crystal where the RBS spectra coincide with the rotating random spectra)

MASTER

REPRODUCTION OF THIS DOCUMENT IS PROHIBITED

DeW

The first objective in our investigation was to employ RBS and ion channeling results in conjunction with the CED model [5] for implantation induced damage production in order to quantify, by a more novel approach, the disordering process during ion implantation of $^{27}\text{Al}^+$ and $^{31}\text{P}^+$ in β -SiC. The Monte Carlo modeling program used in these analyses was TRIM84 [6].

Solid-phase-epitaxial (SPE) regrowth during the thermal annealing of amorphous layers in compound semiconductors has been and continues to be the subject of a host of studies throughout the world [see, e.g.7] and also comprises our second objective in the present research. The quality of these layers is generally very poor even when taking the utmost precautions. The two major problems are that nonstoichiometry results during implantation [8] and that dissociation of the constituent elements of the compound semiconductor generally occurs at different temperatures during thermal annealing. For these reasons, it is pertinent that SPE regrowth of β -SiC be studied.

EXPERIMENTAL

Thin films of monocrystalline (100) β -SiC were epitaxially grown in-house on (100) silicon wafers via chemical vapor deposition [9]. Prior to implantation each sample was mechanically polished, oxidized, and etched in HF in order to obtain a clean, undamaged and smooth surface. The implant energies were 110 keV and 130 keV for the $^{31}\text{P}^+$ and $^{27}\text{Al}^+$ implants, respectively. These implants were produced at room temperature using an offset angle of 7° from the sample surface in order to ameliorate channeling of the implantation beam. The dosimetry was stepwise increased and an RBS spectra taken in order to observe the incremental increase in lattice damage. The residual lattice disorder produced as a result of implantation was analyzed using backscattered energy analysis of 2.5 MeV $^4\text{He}^{++}$ ions incident along the $\langle 110 \rangle$ axial direction. The TRIM84 computer program used to calculate the theoretical damage profiles was executed for both implant species using a threshold displacement energy of 16 eV for SiC. However, it was determined that this parameter could be increased as high as 65 eV for SiC and have little effect on changing the CED for amorphization value.

Amorphous layers were produced in β -SiC by implanting $^{27}\text{Al}^+$, $^{31}\text{P}^+$, and $^{28}\text{Si}^+$, and both $^{28}\text{Si}^+$ and $^{12}\text{C}^+$ in order to study SPE regrowth upon annealing. The purpose of implanting the former two species was to dope β -SiC p-type and n-type, respectively; whereas, the latter two were used for preamorphization

for subsequent dopant introduction at concentrations below which amorphization occurs. A summary of implant species and conditions is given in Table 1. Solid-phase-epitaxial regrowth of amorphized layers was achieved by thermally annealing samples in 1 atm. of Ar at 1600, 1700, or 1800°C for 300s. Annealing in this temperature range has been found to be necessary for optimizing electrical characteristics of implanted p-type and n-type layers in β -SiC [10]. Visual evaluation of the residual lattice damage in the surface implanted regions before and after annealing was conducted using cross-sectional transmission electron microscopy (XTEM). The procedure for XTEM sample preparation is discussed in ref.11.

RESULTS AND DISCUSSION

RBS/Channeling and TRIM84 Analyses

The RBS spectra of Fig. 1a illustrates the accumulation of damage in β -SiC implanted with $^{31}\text{P}^+$ using a grazing angle geometry. Prior to implantation, a virgin and a rotating random spectra were recorded which provided the two analysis limits; an undamaged and an amorphous surface, respectively. Clearly, as the implant dose increased, the damage accumulated until the aligned spectra and the random spectra became coincident. It was determined that this initially occurs when implanting a dose greater than $3.0 \times 10^{14} \text{ cm}^{-2}$ but less than $5.0 \times 10^{14} \text{ cm}^{-2}$. At the latter dose a buried amorphous layer ranging in depth between 55 nm and 118 nm resulted. Implanting at a dose of $3.0 \times 10^{15} \text{ cm}^{-2}$ resulted in a surface amorphous layer 154 nm deep as indicated in the spectra.

In order to determine the CED for amorphization in β -SiC, the above amorphous depth values (as well as others not shown) along with the respective implant doses used to create them, were used in conjunction with the theoretical damage-energy profile shown in Fig. 1b obtained using TRIM84. Both the theoretical and experimental profiles of damage energy density in eV/Å as a function of ion penetration of $^{31}\text{P}^+$ in SiC are represented. The ordinate values for the theoretical curve are absolute as output from TRIM84. However, the ordinate values for the experimental curve have been scaled in order that the two profile peaks occur at the same height [12]. This scaling factor is the CED value for amorphization in β -SiC. This value was determined to be $15.5 \times 10^{23} \text{ eV/cm}^3$ or 16 eV/atom for room temperature.

Fig. 2a shows the RBS spectra for damage accumulation as a result of room temperature implantation of $^{27}\text{Al}^+$ in β -SiC. Again, a virgin and rotating random spectra were obtained for reference. The damage increased rapidly with increasing dose levels above $1.0 \times 10^{14} \text{ cm}^{-2}$. It was determined that the sample became amorphous between dose levels of $4.0 \times 10^{14} \text{ cm}^{-2}$ and $6.0 \times 10^{14} \text{ cm}^{-2}$. No intermediate implant dose was conducted. For the $6.0 \times 10^{14} \text{ cm}^{-2}$ implant, a buried amorphous layer ranging in depth from 70 nm to 168 nm resulted. A surface amorphous layer 213 nm in depth resulted from implanting with a dose of $2 \times 10^{15} \text{ cm}^{-2}$ as illustrated.

The theoretical and experimental damage-energy profiles for $^{27}\text{Al}^+$ in β -SiC were compared using the same method as for the $^{31}\text{P}^+$ implant described above. In this instance, the ordinate scaling factor and thus the CED for amorphization was $15.0 \times 10^{23} \text{ eV/cm}^3$ or 15.5 eV/atom (Fig. 2b). As expected, the amorphizing energy obtained from both analyses was nearly identical. However, deviation between the theoretical and experimental profile depths was quite significant for both implanted species indicating a need for revision of parameters in the TRIM84 program for the implantation of SiC.

Solid-Phase-Epitaxial Regrowth

Figure 3 shows an XTEM micrograph of an $^{27}\text{Al}^+$ double implant region having a peak concentration of $1 \times 10^{20} \text{ Al/cm}^3$. A buried amorphous layer having a crystalline cap of ~ 10 nm thickness resulted after implantation (Fig. 3a). The lower amorphous/crystalline (a/c) interface located at a depth of ~ 170 nm is very diffuse as a result of implanting at room temperature. After annealing at 1600°C for 300s in Ar, the amorphous layer had regrown (Fig. 3b) by SPE. However, a high concentration of defects was observed. Precipitates and/or dislocation loops formed where the upper and lower a/c interfaces were initially located. A broad band of defects (40 nm - 110 nm) resulted where the two a/c interfaces converged during SPE regrowth. In contrast, by annealing a like sample at 1800°C (see Fig. 3c) many of the precipitates did not appear. In this instance, a virtually defect free surface region (0-50 nm) resulted. Additionally, a band containing loops and stacking faults formed at the regrowth convergence as well as small loops where the lower a/c interface was initially located.

Figure 4 illustrates the regrowth properties of a $^{31}\text{P}^+$ double implant with a peak concentration of $1 \times 10^{20} \text{ P/cm}^3$. The annealing temperature was

1700°C. Clearly, the supersaturation of P in the SiC matrix became sufficiently high to cause the layer to regrow in a polycrystalline condition after the first 100 nm of regrowth. However, within the first 100 nm, many small precipitates and loops formed. The regrowth properties of amorphous layers obtained using a lower atomic concentration of P is presently being investigated.

In order to preamorphize β -SiC for subsequent dopant introduction, implantation of $^{28}\text{Si}^+$ and $^{28}\text{Si}^+$ plus $^{12}\text{C}^+$ was conducted. Figure 5 shows an XTEM micrograph of a $^{28}\text{Si}^+$ triple implant region prior to and after thermal annealing. The peak concentration of Si was $1 \times 10^{20} \text{ Si/cm}^3$. After implantation, an amorphous surface layer 440 nm in depth was observed. After annealing at 1700°C for 300 seconds in Ar, the layer regrew epitaxially. The first 70 nm regrew moderately defect free. Thereafter, severe microtwinning and faulting occurred resulting in a polycrystalline layer (Fig. 5b) with a highly preferred orientation.

The XTEM micrographs in Fig. 6 directly compare the structural regrowth properties of implanted and amorphized layers created using $^{28}\text{Si}^+$ and $^{28}\text{Si}^+$ plus $^{12}\text{C}^+$. Figure 6a shows the amorphous layer which was formed by the $^{28}\text{Si}^+$ triple implant with a peak concentration of $3 \times 10^{19} \text{ Si/cm}^3$. The a/c interface is located 400 nm below the sample surface. After annealing at 1700°C for 300s in Ar, the layer regrew epitaxially without severe faulting and/or microtwinning as was observed in Fig. 5b. However, a high concentration of precipitates and/or loops formed throughout the regrown bulk. In an attempt to eliminate these defects, a triple $^{12}\text{C}^+$ implant was superimposed on the triple $^{28}\text{Si}^+$ implant thus simulating implantation of SiC into SiC. The projected range peaks were matched (1:1) SiC in order to obtain the correct stoichiometry using LSS theory. Fig. 6c shows an XTEM micrograph of the regrown layer previously implanted and amorphized with SiC at a peak concentration of $3 \times 10^{19} \text{ implanted SiC/cm}^3$. The annealing conditions were the same as described for the sample shown in Fig. 6b. Quite clearly, implanting $^{28}\text{Si}^+$ plus $^{12}\text{C}^+$ did not structurally improve the quality of the regrown layer. In fact, microfaulting and microtwinning occurred upon regrowth from 140 nm to the sample surface. However, a recent investigation using secondary ion mass spectroscopy has revealed that implants of $^{30}\text{Si}^+$ and $^{13}\text{C}^+$ in SiC do not follow LSS theory and in fact, the above $^{28}\text{Si}^+$ and $^{12}\text{C}^+$ implant profiles may have deviated significantly. Therefore, the authors are further investigating the implantation of both $^{30}\text{Si}^+$ and $^{13}\text{C}^+$ in SiC in an attempt to subsequently improve the character of the regrown implanted layer.

CONCLUSIONS

Using RBS/channeling and the TRIM84 computer code it has been determined that the critical energy for amorphization of β -SiC at room temperature is 16 eV/atom. Furthermore, it has been shown that amorphous SiC undergoes SPE regrowth upon thermal annealing at as low as 1600°C. For the case of amorphous layers created by $^{31}\text{P}^+$ implants, polycrystalline regrowth was observed. Layers implanted with $^{27}\text{Al}^+$ and $^{28}\text{Si}^+$ regrew as single crystals but with residual line and planer defects. Initial attempts have shown that overlaying $^{13}\text{C}^+$ on $^{28}\text{Si}^+$ does not improve the regrowth properties of amorphous SiC.

ACKNOWLEDGEMENT

The authors gratefully acknowledge the support of this program by the Office of Naval Research under contract N00014-82-K-0182 P005 and to the ONR Fellowship program for support of one of the authors (Edmond). *Work at Oak Ridge was sponsored by the Division of Materials Sciences, U.S. Department of Energy under contract DE-AC05-84OR21400 with Martin Marietta Energy Systems, Inc.*

- REFERENCES
- [1] R.R. Hart, H.L. Dunlap, and O.J. Marsh, *Rad. Effects* 9, 261 (1971).
 - [2] J.M. Williams, C.J. McHargue, and B.R. Appleton, *Nucl. Instr. and Meth.* 209/210, 317 (1983).
 - [3] I. Manning and G.P. Mueller, *Comp. Phys. Comm.* 7, 85 (1974).
 - [4] J.P. Biersack and L. G. Hagmark, *Nucl. Instr. and Meth.* 174, 257 (1980).
 - [5] J.R. Dennis and E.B. Hale, *J. Appl. Phys.* 49, 1119 (1978).
 - [6] *J.P. Biersack, W. S. K. Lee, J. Appl. Phys. 51, 772 (1981)*
 - [7] J.P. Donnelly, *Nucl. Instr. and Meth.* 182/183, 553 (1981).
 - [8] L.A. Christel and J.F. Gibbons, *J. Appl. Phys.* 52, 5050 (1981).
 - [9] H.P. Liaw and R.F. Davis, *J. Electrochem. Soc.* 132, 642 (1985).
 - [10] J.A. Edmond, H.J. Kim, and R.F. Davis, to be published in *Materials Research Society symposia Proceedings, Symposium B, Fall, 1985*.
 - [11] C.H. Carter, Jr., J.A. Edmond, J.W. Palmour, J. Ryu, H.J. Kim, and R.F. Davis
 - [12] W. Maszara, G.A. Rozgonyi, L. Simpson, and J.J. Wortman, to be published in *Materials Research Society Symposia Proceedings, Symposium A, Fall, 1985*.

Table I. Summary of ion implantation conditions for SPE regrowth study.
 All implants performed using an offset angle of 7°.

FIGURE NO	ION SPECIES	ENERGIES(keV)	DOSES (cm ⁻²)	PEAK CONC.(cm ⁻³)	IMPLANT TEMP.
3	²⁷ Al ⁺	110,190	6E14,9E14	1E20	RT
4	³¹ P ⁺	110,220	6E14,1E15	1E20	LN ₂
5	²⁸ Si ⁺	80,160,320	6E14,1E15,2E15	1E20	LN ₂
6	²⁸ Si ⁺	120,160,320	2.3E14,3.2E14,5.1E14	3E19	LN ₂
	¹² C ⁺	50,67,141	2.7E14,3.2E14,4.8E14	3E19	LN ₂

2.5 MeV He Analysis of RT P-Implanted Beta SiC

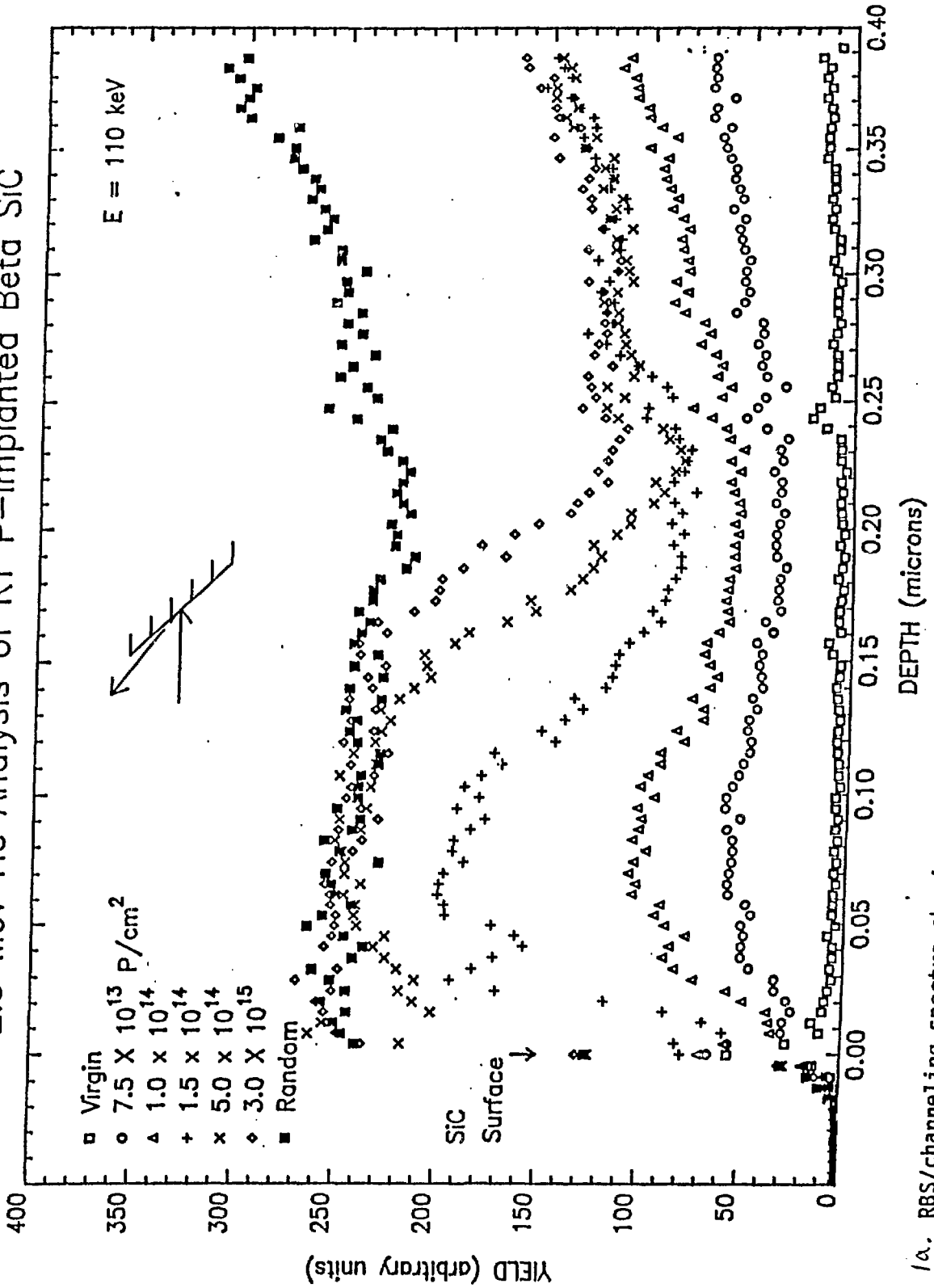


Figure 1/a. RBS/channeling spectra showing the accumulation of damage with an increasing P dose in β -SiC along the $\langle 110 \rangle$ axial direction.

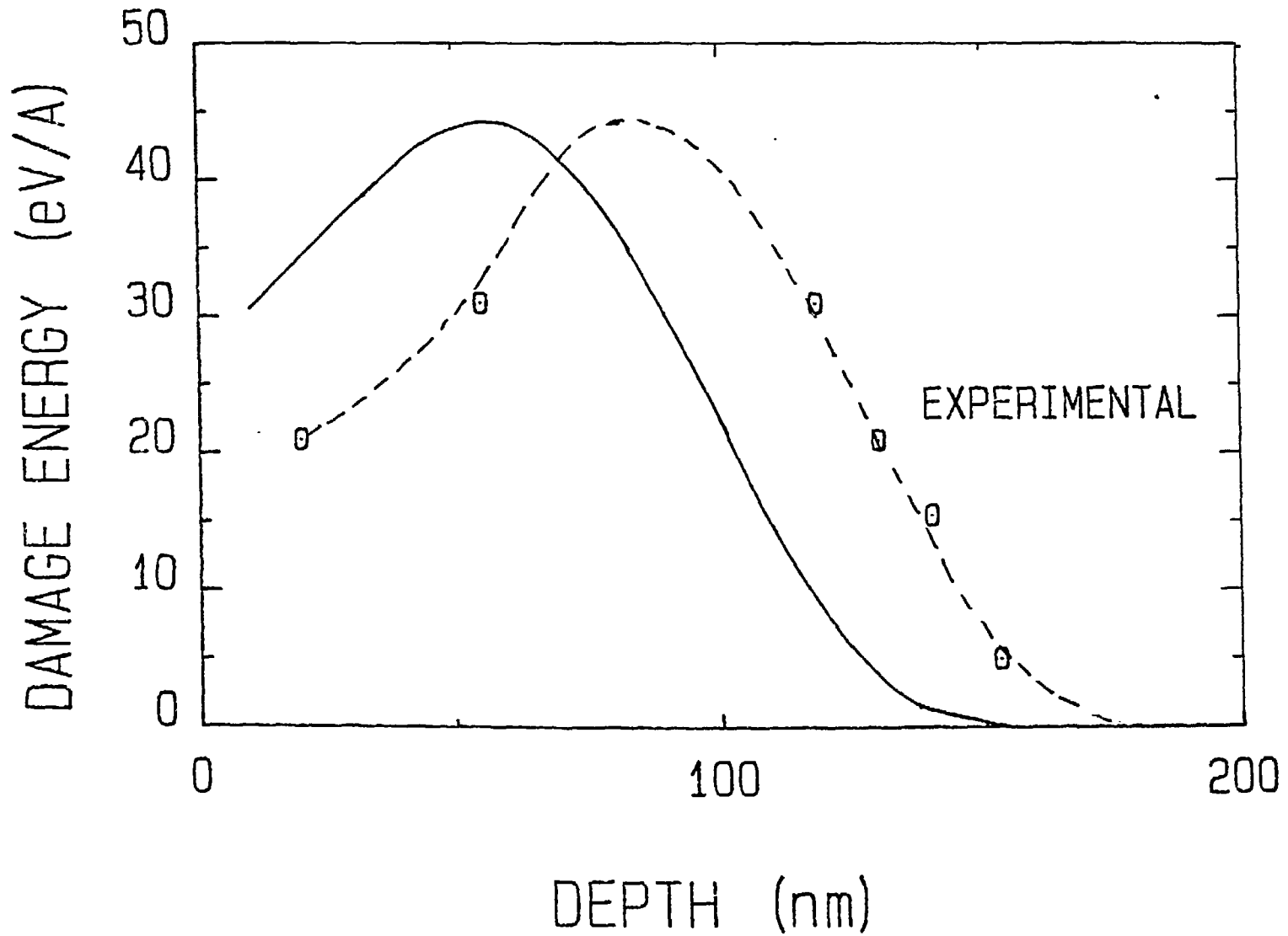


Fig. 1b. Comparison between theoretical (TRIM84) and experimental damage-energy profiles for 110 keV P-implanted Beta SiC

2.5 MeV He Analysis of RT Al-Implanted Beta SiC

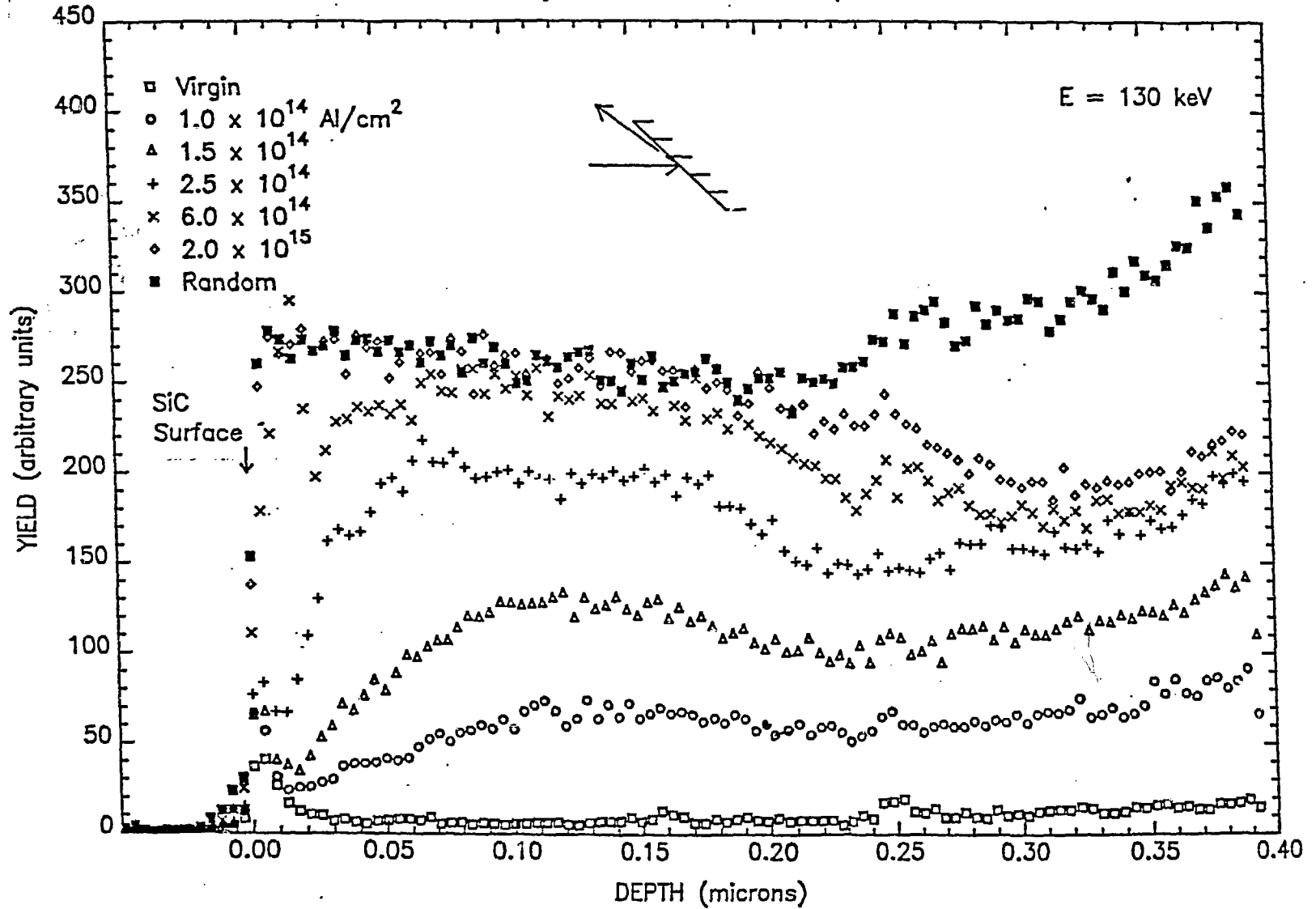


Figure 2a. RBS/channeling spectra showing the accumulation of damage with an increasing Al dose in β -SiC along the $\langle 110 \rangle$ axial direction.

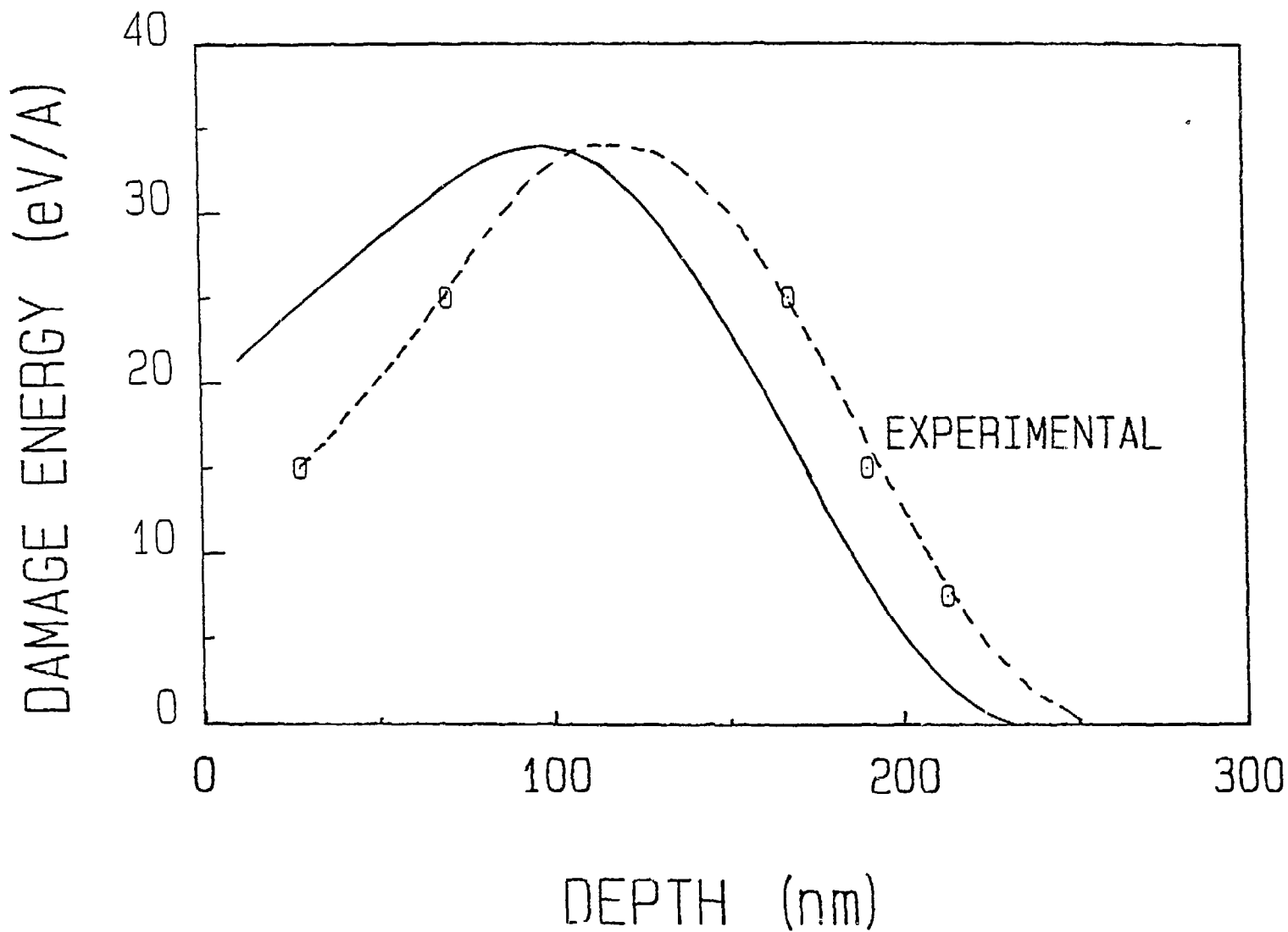


Fig. 2b. Comparison between theoretical (TRIM84) and experimental damage-energy profiles for 130 keV Al-implanted Beta SiC.

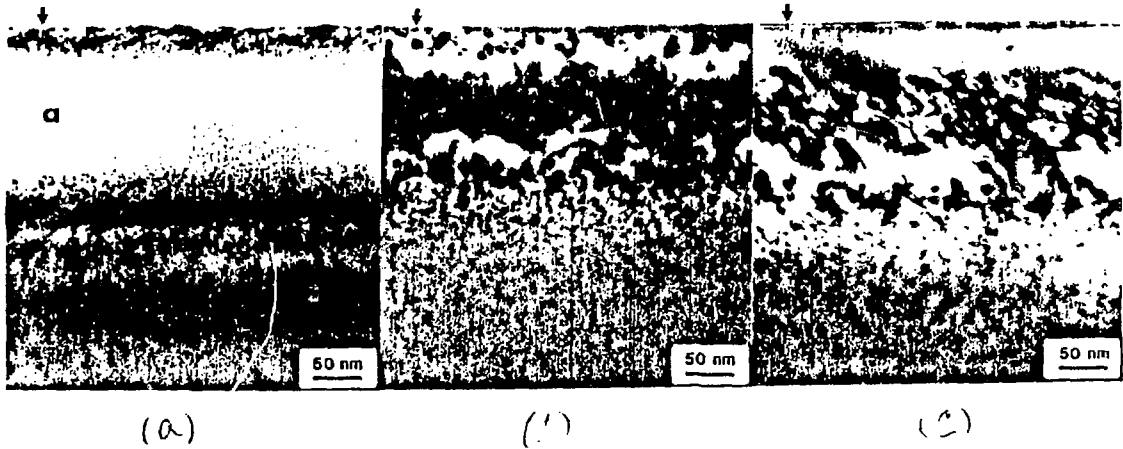


Figure 3. XTEM micrographs showing the surface of a sample which has been double implanted with Al to a peak concentration of 1×10^{20} Al/cm³. (a) As-implanted; (b) annealed at 1873K; (c) annealed at 2073K for 300s.

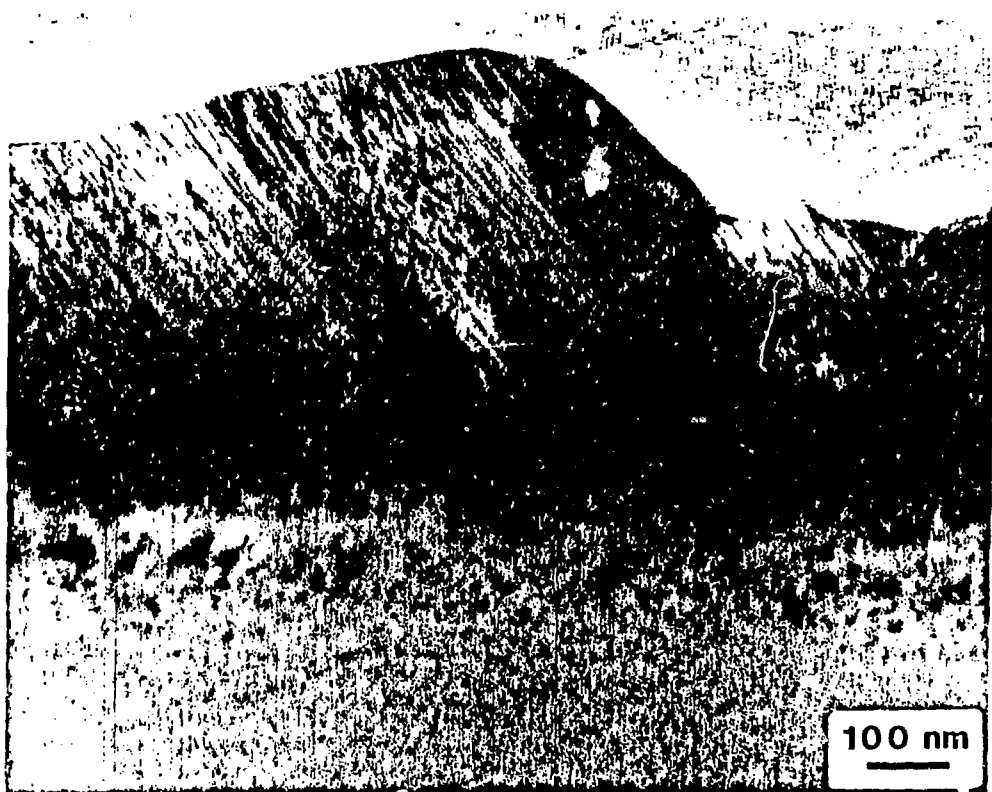
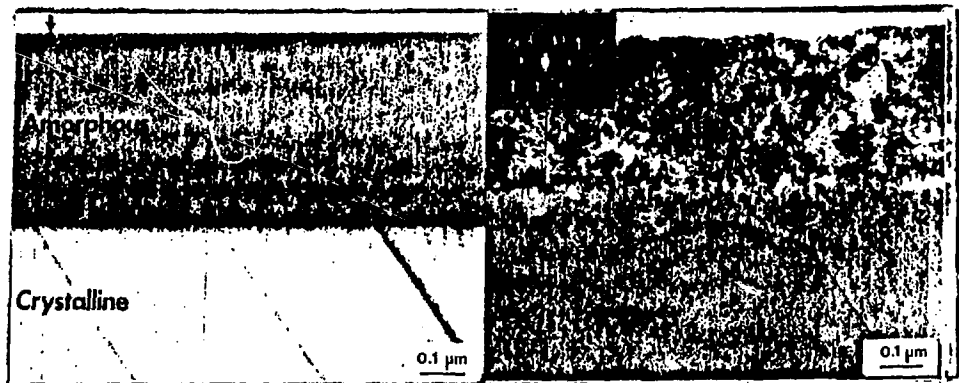


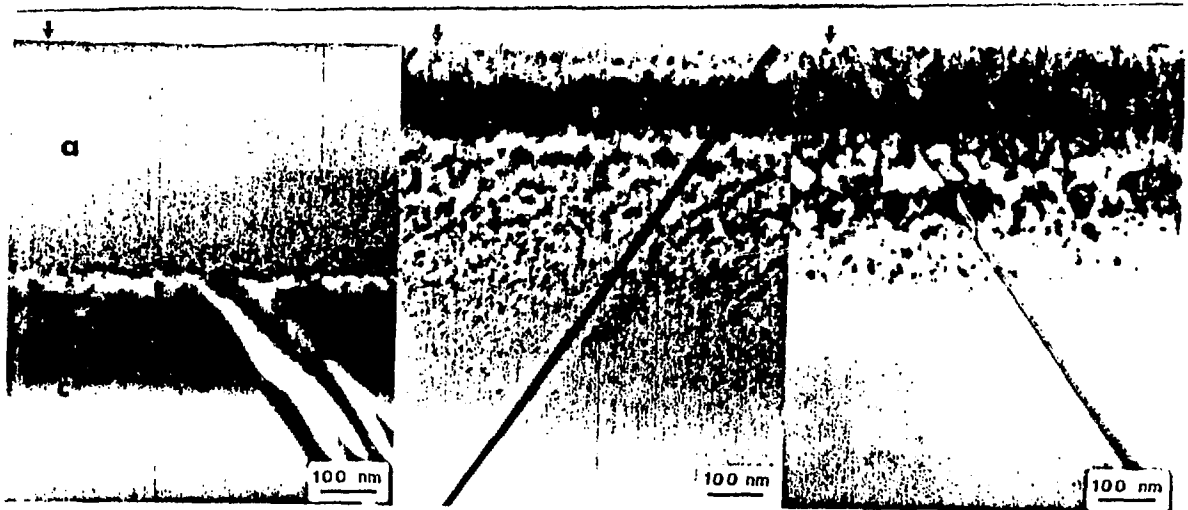
Figure 4. XTEM micrograph of a sample which has been double implanted with P to a peak concentration of 1×10^{20} P/cm³ and subsequently annealed at 1973K for 300s. The surface appears rough as a result of polycrystalline regrowth.



(a)

(b)

Figure 5 XTEM micrographs and diffraction pattern of (100) β -SiC which has been triple implanted with Si to a peak concentration of 1×10^{20} Si/cm³. (a) As-implanted; (b) annealed at 1973K for 300s. (The diffraction pattern is near [011] and of the microtwinning and highly faulted layer).



(a)

(b)

(c)

Figure 6. XTEM micrographs comparing the regrowth properties of samples implanted with equal atom concentrations (3×10^{19} /cm³) of Si (b, center) and Si + C (c, right). The as-implanted amorphous layer is also shown (a).